

Supplement of Atmos. Chem. Phys., 15, 11047–11066, 2015  
<http://www.atmos-chem-phys.net/15/11047/2015/>  
doi:10.5194/acp-15-11047-2015-supplement  
© Author(s) 2015. CC Attribution 3.0 License.



*Supplement of*

## **An empirically derived inorganic sea spray source function incorporating sea surface temperature**

**M. E. Salter et al.**

*Correspondence to:* M. E. Salter ([matthew.salter@aces.su.se](mailto:matthew.salter@aces.su.se))

The copyright of individual parts of the supplement might differ from the CC-BY 3.0 licence.

## 1 Artificial seawater oxygen supersaturation

The second phase of the experiment consisted of measurements of the aerosol generated whilst the temperature of the water was slowly ramped downward from 30 °C to 2 °C over a period of 29 h. Figure 1 plots the evolution of the seawater temperature and O<sub>2</sub> % saturation during the temperature ramp experiment. A relatively rapid decrease in the supersaturation of O<sub>2</sub> is evident after the seawater cooling process was initiated. Following this initial period the oxygen saturation slowly increased to its value prior to the initiation of the cooling process. At no point during the seawater cooling experiment was the water undersaturated with respect to O<sub>2</sub>, nor was it significantly different than the mean of the constant temperature experiments (111 %).

## 2 Temperature ramp size distributions

Figure 2 plots the particle size distributions from the temperature ramp experiments.

## 3 Effective vs. interfacial sea spray aerosol fluxes

The aim of this study is to provide a parameterisation of sea spray aerosol production to represent the production flux in atmospheric chemical transport models/global circulation models. Usually such models have their lowest atmospheric layer at heights well above the ocean surface. Therefore, knowledge of the size distribution of particles that attain this height (often referred to as the effective flux) is required. Since the inlets to the aerosol instrumentation used during this study were sited ~30 cm above the water surface we have determined the flux of particles that reached this height, often referred to as the interfacial flux. As such, consideration should be given to the difference between the effective production flux and the interfacial production flux measured at ~30 cm.

The mechanisms controlling the heights sea spray aerosol particles attain are turbulent diffusion, parameterised by the eddy diffusion coefficient  $D_{\text{eddy}}$ , which is assumed independent of particle size, and gravitational sedimentation, parameterised by  $v_{\text{term}}$ .  $v_{\text{term}}$  depends on the geometric radius of the particle and its density, and can be obtained by equating the drag force with the gravitational force on the particle through the Stokes velocity  $v_{\text{stk}}$ :

$$v_{\text{stk}} = \frac{2}{9} \frac{(\rho_p - \rho_a)}{\rho_a} \frac{g}{v_a} r^2 C \quad (1)$$

where  $\rho_p$  is the density of the particle,  $\rho_a$  is the density of air,  $g$  is the acceleration due to gravity,  $v_a$  is the kinematic viscosity of air,  $r$  is the geometric radius of the particle, and  $C$  is the Cunningham slip factor. For neutrally stable atmospheric conditions,  $D_{\text{eddy}}$  is directly proportional to the height above the water surface ( $z$ ) and the size dependent concentration profile that results is described by a power law in height:

$$\frac{n(z)}{n(z_1)} = \frac{z}{z_1}^{-\frac{v_{\text{term}}}{k u_*}} \quad (2)$$

where  $k$  is the von Karmen constant (0.4) and  $u_*$  is the wind friction velocity:

$$u_* = \sqrt{C_D U_{10}} \quad (3)$$

where  $C_D$  is the dimensionless wind stress coefficient (0.0013 is used in this study).

Consideration of this size dependent concentration profile can be used to obtain a quantitative estimate of the size dependence of the ratio of the effective sea spray aerosol production flux to the interfacial sea spray aerosol production flux,  $\Phi_f(D_p)$ , and its dependence on dry diameter and wind speed. This ratio, calculated using Eq. 2 for a series of wind speeds, is shown in Fig. 3 as a function of dry diameter. We have used this ratio to correct our measured interfacial fluxes to effective fluxes throughout this study.

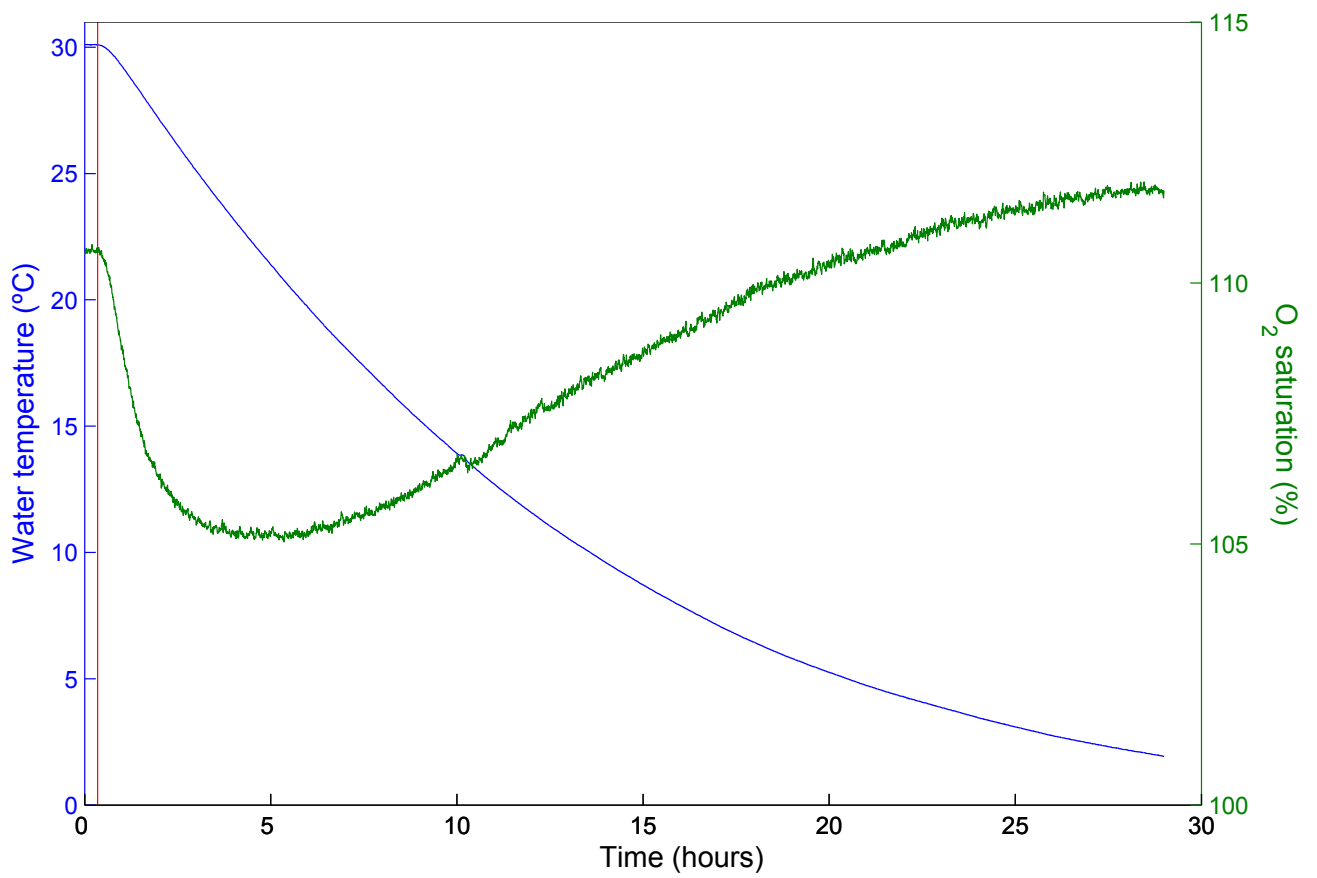


Figure 1: The evolution of the water temperature and O<sub>2</sub> % saturation during the temperature ramp experiment. The vertical red line signifies the point at which the cooling of the water was started.

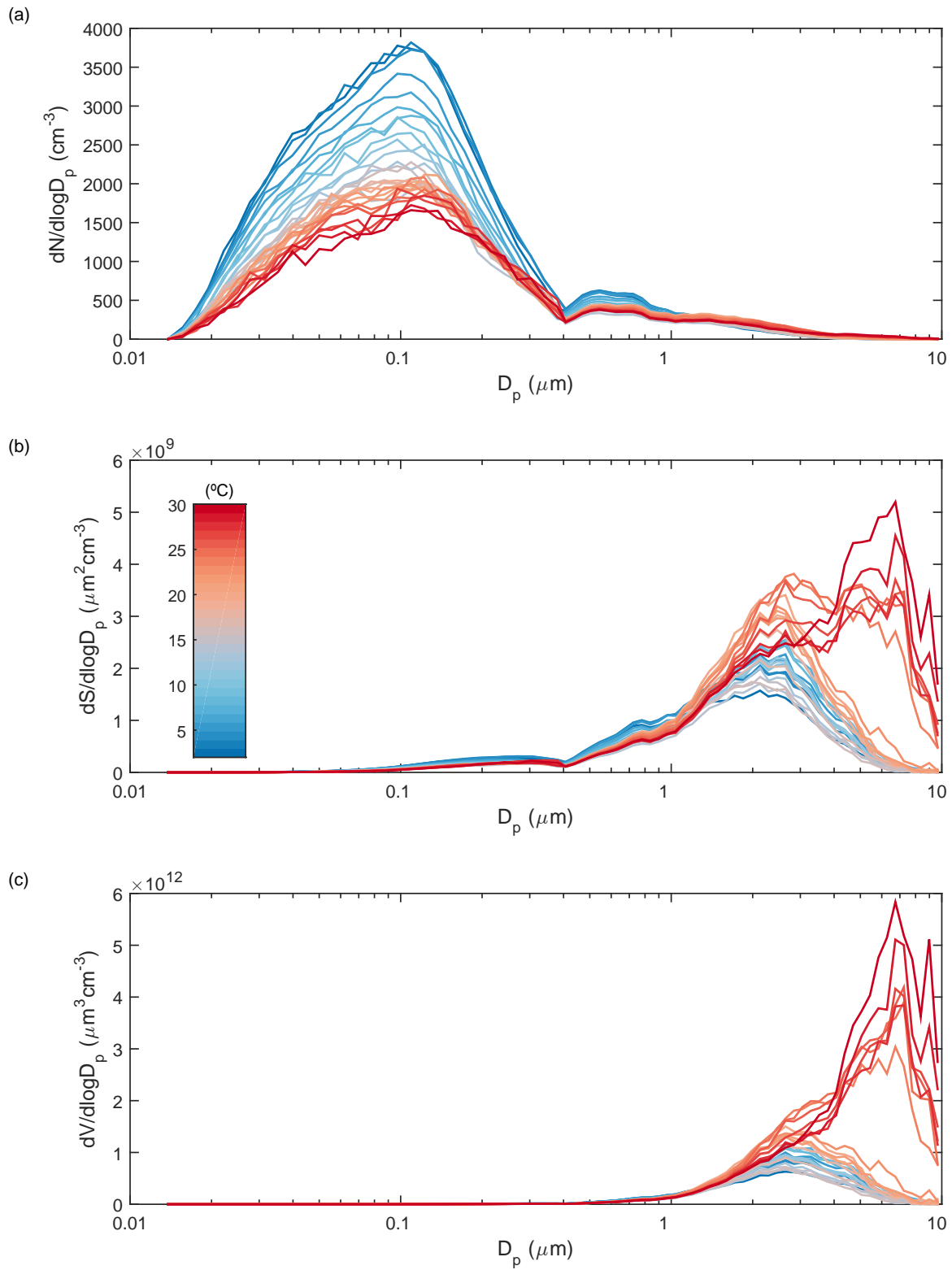


Figure 2: Mean particle **a)** number size distribution, **b)** surface size distribution, and **c)** volume size distribution measured at different water temperatures during the temperature ramp experiment.

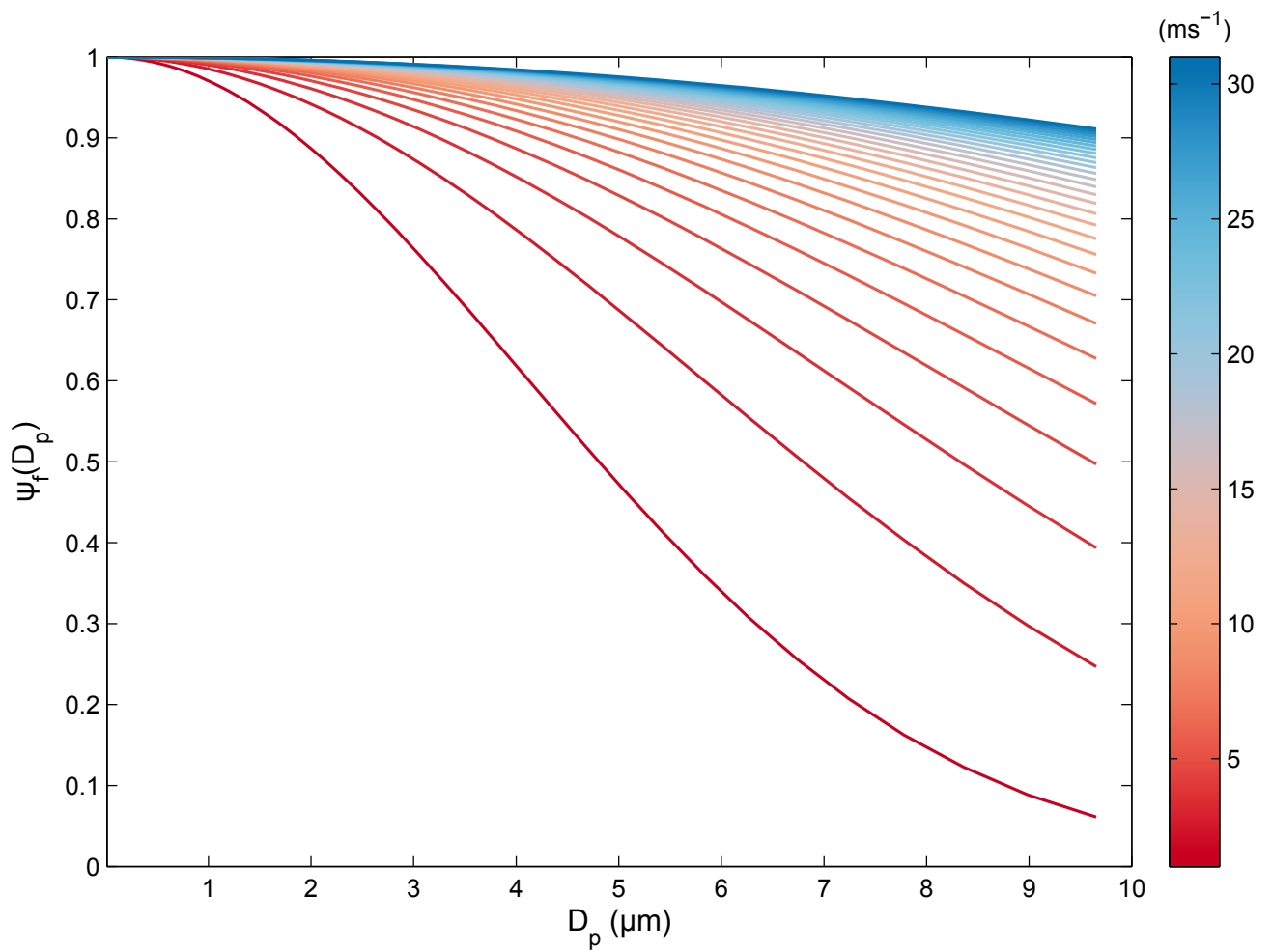


Figure 3: Ratio of the effective flux at 10m to the interfacial production flux measured in the laboratory at  $\sim 30$  cm for conditions of neutral stability and a series of wind speeds between  $1 \text{ m s}^{-1}$  to  $30 \text{ m s}^{-1}$ .